Accounting for the Effects of Dislocation Climb Mediated Flow in Mg Alloy ZK10 Sheet

Michael A. Ritzo and Sean R. Agnew

Abstract

Tensile samples of an Mg alloy ZK10 sheet were tested at a range of temperatures and strain rates designed to rather evenly probe a range of Zener Hollomon parameter values, from ln(Z) ≈ 15 (10^{-4} s^{-1} and 623 K) up to ln(Z) ≈ 50 (10^{-3} s^{-1} and 300 K). In contrast with more commonly examined Mg alloy AZ31B sheet material, ZK10 sheet material shows modest strain anisotropy (r-value) at low temperatures for both 45° ($r_{45} \approx 1.2$) and TD ($r_{TD} \approx 1.4$) sample orientations, despite showing evidence of significant prismatic slip of <a> dislocations, which often leads to high r-values at low temperatures. These low r-values become even lower ($r_{45} \approx 0.84$ and $r_{TD} \approx 0.89$) at high temperatures. These behaviors are hypothesized to occur due to a distinct initial texture and deformation mechanism activity, which includes a modest level of tensile twinning and <c + a> slip at both room and elevated temperature. A version of the viscoplastic self-consistent (VPSC) code, which accounts for the kinematics of dislocation climb, is used to simulate the behavior of a textured Mg alloy ZK10 sheet reveals that both the glide of pyramidal <c + a> dislocations and the climb of basal < a > dislocations are required to describe the behavior at elevated temperatures.

Keywords

Texture • Anisotropy • Dislocation • Climb • Twinning • Crystal plasticity

M. A. Ritzo · S. R. Agnew (✉)
Department of Materials Science and Engineering, University of Virginia, 22904 Charlottesville, VA, USA
e-mail: agnew@virginia.edu

M. A. Ritzo
e-mail: mar3dm@virginia.edu

Introduction

The use of polycrystal plasticity modeling has radically changed our understanding of the deformation of hexagonal close packed (hcp) Mg alloys over the past two decades. Historically, it was believed that $\{10\bar{1}2\}$ tensile twinning was a significant deformation mechanism only at low temperatures. A major reason for this was that the critical resolved shear stress (CRSS) for twinning was shown to be nearly temperature insensitive whereas the CRSSs of the hard, non-basal slip mechanisms (i.e., prism <a> and pyramidal <c + a>) tend to be highly temperature sensitive [1–4]. During room temperature deformation, $\{10\bar{1}2\}$ tensile twinning is known to be one of the few mechanisms that can accommodate strains along the <c> axis. Pyramidal slip of <c+a> dislocations, the another slip mode which can accommodate <c> axis strain, has a rather high CRSS value at room temperature, which limits its activity [5] and has led to suggestions that it may be more important at higher temperatures. Other suggestions include climb of basal <a> and non-basal [c] dislocations, grain boundary sliding, and diffusional flow. The higher stress conditions presently of interest ensure that diffusional flow will not be controlling.

The interplay between deformation twinning and dislocation slip (glide) has been studied in different contexts, but the role of dislocation climb, used to explain differences in texture evolution and r-value of AZ31 has yet to be applied broadly to the high temperature deformation of other Mg alloys, such as ZK10 (the material chosen for the current study), which is known to undergo significant twinning at room temperature [6]. One implication for the current study is that$\{10\bar{1}2\}$ twins have been shown to transmute gliding <a> matrix dislocations into <c + a> dislocations in the twin [7]. <c + a> slip has been thought to reduce the strain anisotropy in Mg alloys and promotes a characteristic texture, distinct from all other slip modes. The possible influence of twinning in the activation of <c + a> glide at high

V. M. Miller et al. (eds.), *Magnesium Technology 2021*, The Minerals, Metals & Materials Series,
https://doi.org/10.1007/978-3-030-65528-0_6

temperature is of great interest, as <a> climb has been shown to be competitive with non-basal slip modes, particularly <c + a> glide on second order pyramidal planes [8].

Dislocation climb and cross-glide are relevant to applications involving creep, load relaxation (such as bolt-load retention), and hot/warm forming operations. Indeed, the measured constitutive response of Mg and its alloys frequently exhibits power-law type constitutive behavior at temperatures and rates relevant to these applications (e.g., [1]). Rarely have crystal plasticity modelers accounted for these aspects, though the work of Staroselsky and Anand [2] notably considered the possible role of grain boundary sliding. In addition, the interplay between twinning and dislocation climb at high temperatures has not been studied previously.

Only recently has it become possible to explore the unique characteristics of Mg alloy ZK10. Several crystal plasticity models for describing twinning in polycrystalline materials have been developed, but no such models existed to predict the effect of dislocation climb on texture and strain anisotropy. A viscoplastic self-consistent (VPSC) polycrystal modeling code, which accounts for the non-conservative (climb) motion of dislocations has been developed recently, [8, 9] which will allow for the simultaneous study of twinning and climb.

We begin by providing a brief introduction to the climb and twinning models, followed by a description of experimental methods and results which highlight the effects we are hoping to explain, and then enumerate simulation results that explore the effect of tension twinning on the relative activities of slip and climb modes. The tensile deformation of ZK10 was studied as its unique rolled texture made it a model system to explore the effect of twinning. Tensile deformation parallel to and 45° away from the sheet transverse direction is considered to study the effect of sample orientation on the twin volume fraction.

Modeling Background

Crystal plasticity models generally consider dislocation glide and twinning [10, 11] as the only dissipative processes. In addition, both slip and twinning are assumed to be governed by the generalized Schmid law, which resolves the stress $\boldsymbol{\sigma}$ on the slip system as follows:

$$\tau = m : \sigma \tag{1}$$

where $\mathbf{m} = \mathrm{sym}\left(\hat{\mathbf{b}} \otimes \hat{\mathbf{n}}\right)$ is the Schmid tensor, $\hat{\mathbf{n}}$ is the slip plane normal and $\hat{\mathbf{b}}$ is the slip direction [13]. The role of cross-slip is often associated with the process of dynamic recovery [14], and the role of dislocation climb treated similarly. The strain accommodated by these mechanisms is for the most part disregarded. Lebensohn et al. [9] generalized the connection between stress and dislocation motion, beyond the Schmid law of Eq. 1. by appealing to the full Peach–Koehler relationship,

$$f = (\boldsymbol{\sigma} \cdot \mathbf{b}) \times \hat{\mathbf{t}} \tag{2}$$

where $\mathbf{b}$ is the Burgers vector and $\hat{\mathbf{t}}$ is the dislocation line direction. The forces which drive dislocation glide (the Schmid stress times the magnitude of the Burgers vector) can then be parsed from those which drive climb.

$$f_g = \left\{(\sigma \cdot \mathbf{b}) \times \hat{\mathbf{t}}\right\} \cdot \hat{\chi} = \left\{\sigma : \left(\hat{\mathbf{b}} \otimes \hat{\mathbf{n}}\right)\right\}|b| \tag{3}$$

where $\hat{\chi}$ is the direction of dislocation glide (within the glide plane and orthogonal to the line direction). On the other hand, the climb force is resolved along the glide plane normal direction.

$$f_{2c} = \left\{(\sigma \cdot \mathbf{b}) \times \hat{\mathbf{t}}\right\} \cdot \hat{\mathbf{n}} = -\left\{\sigma : \left(\hat{\mathbf{b}} \otimes \hat{\chi}\right)\right\}|b| \tag{4}$$

Notably, the glide force only depends upon the deviatoric stress (the addition of pressure has no effect), whereas the climb force depends on the full stress tensor. For dislocation glide, the dyadic cross product $\hat{\mathbf{b}} \otimes \hat{\mathbf{n}}$ can be decomposed into symmetric (strain, $\mathbf{m}$) and antisymmetric (rotation, $\mathbf{q}$) components. Indeed, this slip-induced rotation is the basis of texture evolution during glide. For climb, the analogous tensor, $\hat{\mathbf{b}} \otimes \hat{\chi}$ can be decomposed into symmetric strain ($\mathbf{k}$) and rotation ($\mathbf{r}$) components. The distinct types of strain and rotation associated with climb and glide provide a means by which their contributions to the deformation may be parsed. For example, the strain rate within a crystal undergoing glide and climb may be expressed as a function of the applied stress as follows.

$$\dot{\varepsilon} = \sum_s \mathbf{m}^s \left(\frac{f^s}{\tau_c^s b^s}\right)^{n_g} \boldsymbol{sign}(\mathbf{m}^s : \boldsymbol{\sigma}) + \sum_s \mathbf{k}^s \left(\frac{f^c}{\sigma^c b^s}\right)^{n_c} \boldsymbol{sign}(\mathbf{k}^s : \boldsymbol{\sigma}) \tag{5}$$

Relative to traditional crystal plasticity, the relations are complicated by the fact that one must track the character of dislocation populations. Indeed the "climb strain tensor," $\mathbf{k} = \mathrm{sym}\left(\hat{\mathbf{b}} \otimes \hat{\chi}\right)$, can be expressed in terms of the angle between the Burgers vector and line direction.

Many approaches have been taken in order to simulate the effect of twinning; the two most important models are the Predominant Twin Reorientation (PTR) [15] and the Twinning Detwinning (TDT) [16] models. In both cases, twinning is activated per the same power-law constitutive rule and Schmid stress as described above for slip. Distinctly, a volume fraction of each activated twin variant created within each straining increment is proportional to the strain accommodated, and the proportionality constant is the characteristic twinning shear of that mode (e.g., $\sim$ 0.14 for the $\{10\bar{1}2\}$ tensile twin). In this early study of the interaction between dislocation climb and twinning, we employ the PTR model which attempts to capture effect of twinning on texture by selectively reorienting grains that surpass a threshold twinning volume fraction (F_T) as defined by Eq. 6

$$F_T = 0.25 + 0.25\frac{F_E}{F_R} \tag{6}$$

When the volume fraction of a grain undergoing twinning exceeds F_T, the grain in question is reoriented according to its most active twin variant. F_E is a measure of the twinning volume fraction calculated by summing the volume fractions of all grains that have been completely reoriented and F_R tracks the total volume fraction of twins which have been invoked and is known as the "real" twinned fraction, as this is akin to the volume fraction that can be measured. The major advantage of this model is computational efficiency, since the number of grains in the calculation remains fixed throughout the simulation. The major disadvantages are that entire grains are reoriented instead of local regions and that the model only accounts for the texture evolution associated with the most active twinning system in each grain.

In this study, the experimentally measured texture is used as an input and boundary conditions appropriate for uniaxial tension parallel to (TD) or 45° away from (45) the sheet transverse direction are imposed. The parameters which were explored include the critical resolved shear strengths (τ) of the prismatic <a>, pyramidal <c + a>, tensile twinning, and basal <a> climb, all relative to the strength of basal <a> slip. The outputs presently under consideration are the r-value and the evolved texture after deformation. The power-law exponents employed in this study were fixed at $\boldsymbol{n_g} = 3$ and $\boldsymbol{n_c} = 3$, for high temperature simulations and $\boldsymbol{n_g} = 20$ for low temperature simulations, though further exploration of the effects of these parameters on the constitutive response and texture evolution is merited.

Experimental Methods

Mg alloy ZK10 sheet with 1 mm thickness was provided by the former Magnesium Elektron North America, part of the Luxfer group, with a nominal composition of 1wt% Zn and 0.5% Zr. The samples were received in the F (as-worked) temper, but examined in the O (soft annealed) temper, which involved annealing at 300 °C for 1 h to fully recrystallize the microstructure. The microstructure of the samples was examined in previous study and found to be comprised of equiaxed grains with a lineal intercept grain size of −10 mμ with only occasional twins from the prior deformation in addition to few precipitates present [6]. The texture is measured using X-ray diffraction from the sheet midplane, both before and after deformation, using a Panalytical X'pert Pro MPD diffractometer, as described previously [17]. The texture analysis and representation were performed using the MTEX toolbox for MATLAB [18]. A preliminary assessment of the twin fractions in deformed samples was made by tracking the orientations on the basal pole figure with tilt values, α > 50° and subtracting them from the orientations collected from the undeformed sample. The process was repeated for α > 80° in order to determine upper and lower bound estimates of the twin fraction.

Tensile samples with an ASTM E-8 sub-sized standard dog bone geometry were prepared from the sheets using electrodischarge machining. The effective gauge section of the samples is approximately 33 mm long by 6 mm wide. The r-values were measured as the ratio of the logarithmic true plastic strains along the width and thickness directions, after deforming the samples to a plastic strain of 0.08–0.12 perpendicular (TD) and 45° (45) to the rolling direction. One test of the accuracy of the strain measurements was to examine volumetric strain implied, and since plasticity is known to be volume constant, only those measurements with implied absolute dilatation of less than ~0.005 were retained in the final analysis.

Tensile tests were performed at temperatures ranging from room temperature up to 350 °C, at strain rates ranging from 10^{-4} to 10^{-3} s^{-1}. The tensile test data were analyzed in terms of the flow stress measured at a plastic strain of ~0.10. The test conditions were chosen in order to obtain a wide range of Zener–Holloman parameter, Z, also known as the temperature-compensated strain rate:

$$Z = \dot{\varepsilon}\exp\left(\frac{Q}{RT}\right) \tag{7}$$

where Q is the activation energy and R is the universal gas constant. Sellars and Tegart [19] suggested a hyperbolic sine function would describe the relationship between rate and flow stress over a wide range of hot working and creep conditions.

$$Z = A\{\sinh(\alpha\sigma)\}^n \tag{8}$$

At low stress (or Z) conditions, this relationship asymptotes to a simple power-law indicative of high temperature creep, whereas it asymptotes to an exponential function of stress at high stresses, which is typical of thermally activated slip. That is, it does a reasonably good job of describing both the power-law and power-law breakdown regimes. The empirical parameters A, α, n, and Q were obtained by least-squares non-linear regression.

Experimental Results

Tensile test results are shown in Fig. 1a. It is clear that increased temperature results in the lowered yield and ultimate tensile stress. In addition, the amount of hardening decreases as the temperature increases. Figure 1b presents the flow stress during uniaxial straining parallel to the TD and between RD and TD, at a tensile plastic strain of ∼ 0.10, plotted as a function of the Zener–Holloman parameter, *Z*. Superimposed on the experimental data is a best-fit Sellars–Tegart function (Eq. 8), with a stress exponent $n = 3.5$. Such a value suggests that the rate-controlling deformation mechanism is dislocation climb at conditions of $Z \sim 22$ or less. The transition to rate-insensitive plasticity (or power-law breakdown) occurs over the range of $22 \leq Z \leq 35$. At even higher Z levels, the plasticity is rate-insensitive. The focus of this study is placed upon examining the texture evolution and strain anisotropy over these same three *Z*-value regimes.

Figure 1b also presents the r-values measured at a plastic tensile strain of 0.08–0.12 and plotted as a function of applied *Z*. In the low Z regime, the r-value is close to 1 (near plastic isotropy) and in the high Z regime, the r-value is ∼1.4. There is a slight difference in r-value between sample orientations at the high Z test conditions that is not present at low Z. It is notable that conditions where the constitutive modeling suggests the onset of significant strain accommodation by dislocation climb (i.e., the low Z power-law climb and glide regime), the r-value begins to decrease.

Finally, the crystallographic texture and its evolution after tensile deformation within each of the aforementioned Z-regimes is presented in Fig. 2. Samples tested at high Z conditions show significant activity of prism dislocations, which is manifests as intensity of the ODF in Rodrigues space forming nodes at the top (for 45° samples) or bottom (for TD samples) of the Z axis. In contrast to previous studies on AZ31B, the ZK10 samples in the current study exhibited dramatically lower r-values, which is attributed to reduced prism slip [17]. This also helps to explain the lower yield stresses of these ZK10 sample at ambient temperatures, since the distinct texture permits the softer basal slip mechanism to accommodate greater fraction of the macroscopic strain. Another possible contributor to decreased r-values could be <c + a> slip on pyramidal planes, which was found to be the dominant deformation mechanism of Mg single crystals oriented for $\langle 11\bar{2}0\rangle$ tension or $\langle 0001\rangle$ compression at ambient temperatures in Mg–Li and Mg–Zn [20], Mg–Y [21] and at high temperatures in Mg–Al–Zn [22] and pure Mg [23]. Notably, only single crystals of Mg–Al–Zn did not show a dominance of <c + a> slip under these straining conditions, suggesting that it is the unusual case, even though it is the most common commercial wrought Mg alloy.

The twin volume fractions were estimated to be between 1.5 and 7.5%, based upon the measured deformation textures, though no clear trend with testing direction or test conditions (Z) is apparent. Due to the minor contribution twinning makes to the overall strain accommodation, even at room temperature, it is not considered to be a significant contributor to the low yield strength of this alloy.

As the temperature is increased (and Z-value is correspondingly decreased), the texture evolution undergoes a transition, whereby the intensity forms two fibers along the z axis. In the low Z regime, where the r-value is decreased below 1, the texture appears similar to the undeformed texture, i.e., the deformation texture evolution is greatly slowed at low Z conditions (Fig. 3a). Previous study of Mg alloy AZ31B revealed that this is due to the activation of basal <a> dislocation climb, which does not cause rotations in the texture and, therefore, results in a slowing of the texture evolution which would otherwise occur due to dislocation glide.

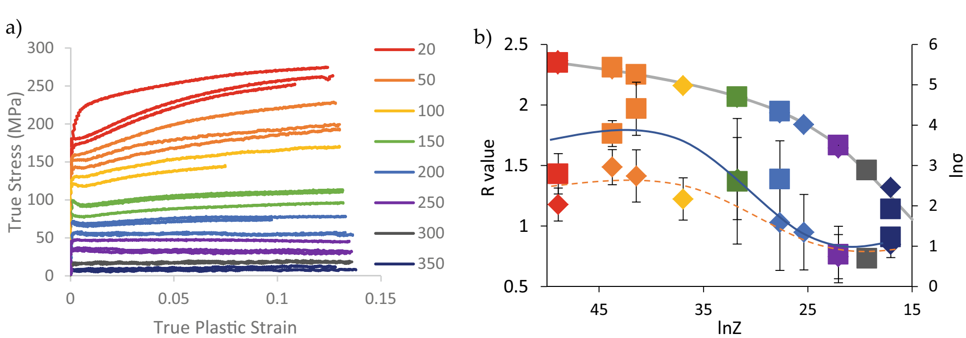

Fig. 1 **a** Stress–strain plots performed from ambient to 350 °C. **b** Plot of log-flow stress vs. log-Z (right y axis). The r-value for samples of textured Mg alloy, ZK10, sheet material tested parallel to the sheet transverse direction (TD) and 45° away from TD (left y axis). The solid (TD data) and dashed (45° data) curves are meant to guide the eye, but suggests three mechanistic regimes at low, intermediate, and high Z-values. (Color figure online)

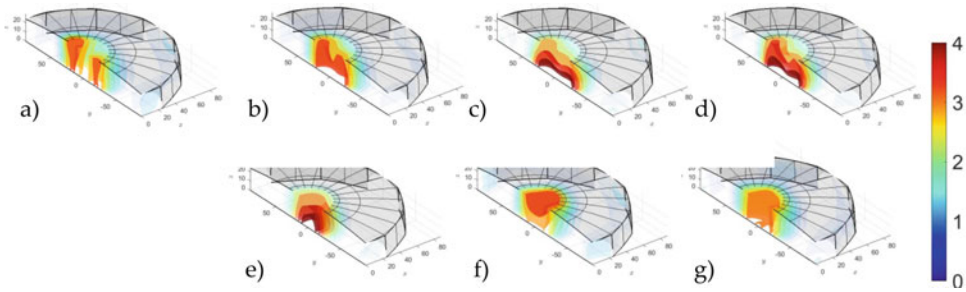

Fig. 2 Crystallographic textures of samples Mg alloy ZK10 sheet material tensile tested parallel to the transverse direction (TD) (**a**–**d**) and 45° away from it (45) (**e**–**f**). The textures correspond to (**a**) undeformed and deformed at ln Z = (**b & e**) 48.9, (**c & f**) 31.8, and (**d & g**) 19.3 (**d & h**). Unless provided, all ODFs share the same scale as Fig. 2. (Color figure online)

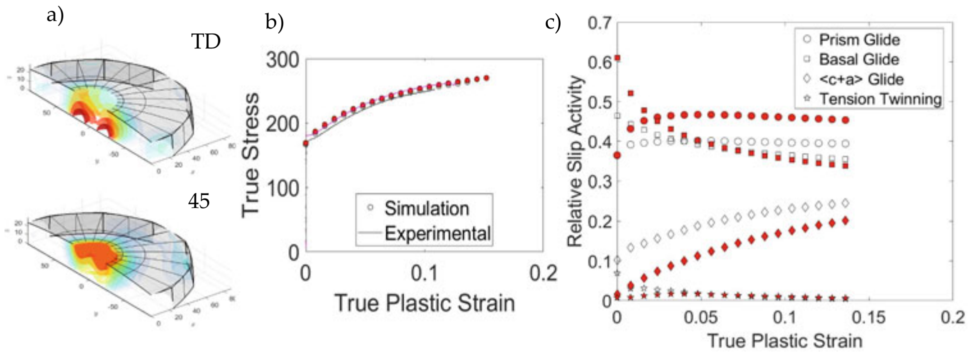

Fig. 3 Low temperature **a** TD and 45° orientations textures. **b** Experimental and simulated stress–strain curves of TD and 45° samples. **c** Relative slip activity plots of simulated tensile tests. Closed symbols and lighter lines represent TD samples and opened symbols and darker lines represent 45° samples. (Color figure online)

Modeling Results

Numerous authors have explored the effects of varying the critical resolved shear stress (CRSS) ratios of basal, prismatic <a>, and pyramidal <c + a> slip can have on the r-values and texture evolutions [e.g., 3]. Here we focus on the effects of climb of basal <a> type dislocations on a twinning prone alloy. Figure 3 shows the optimized set of Voce parameters used to simulate the low temperature tensile tests. It is clear from Fig. 3c that in both sample orientations that the majority of the strain is accommodated through basal and prism glide, which is expected for low temperature deformation. Tensile twinning has a low relative activity, which is related to the low twinning fractions estimated experimentally. Surprisingly, <c + a> glide has significant activity at ambient temperatures in both orientations and may explain the lower r-values of the 45° sample orientation as increased <c + a> glide activity. This is in contrast to the previously mentioned study on AZ31B, where the glide of <c+a> dislocations on second order pyramidal planes was suppressed at low temperatures. This could be due to alloy chemistry as it was shown that Al and Zn additions to single crystal Mg samples increase the CRSS of <c + a> glide and decrease the twinning CRSS [22]. Curiously, it does not seem to have a strong effect on the alloy's ductility as one would predict.

In order to simulate the high temperature experimental samples, large batches of simulations were performed with varying the CRSS values which control tension twinning, prism <a> and second order pyramidal <c + a> glide, along with the critical stress which controls the climb of basal <a> dislocations (all relative to the CRSS of basal <a> glide). Equations 9 and 10 were used to quantify the total residual error between the experiments and simulations, taking into account the plastic anisotropy (r-values) and deformation texture of both sample types.

$$RelErr = TexErr_{TD} + \frac{\left|r_{sim} - r_{exp}\right|_{TD}}{r_{TD\_exp}} + TexErr_{45} + \frac{\left|r_{sim} - r_{exp}\right|_{45}}{r_{45\_exp}} \tag{9}$$

$$TexErr = \sqrt{\int \left(f_{exp}(g) - f_{sim}(g)\right)^2 dg} \tag{10}$$

where $f_{exp}(g)$ and $f_{sim}(g)$ refer to the orientation distribution functions of the experimental and simulated deformation textures, respectively.

Fig. 4 Top: **a**–**c** Constant prism CRSS (P/B = 1) and Bottom: **d**–**f** Constant tension twinning CRSS (TT/B = 1.3). (Color figure online)

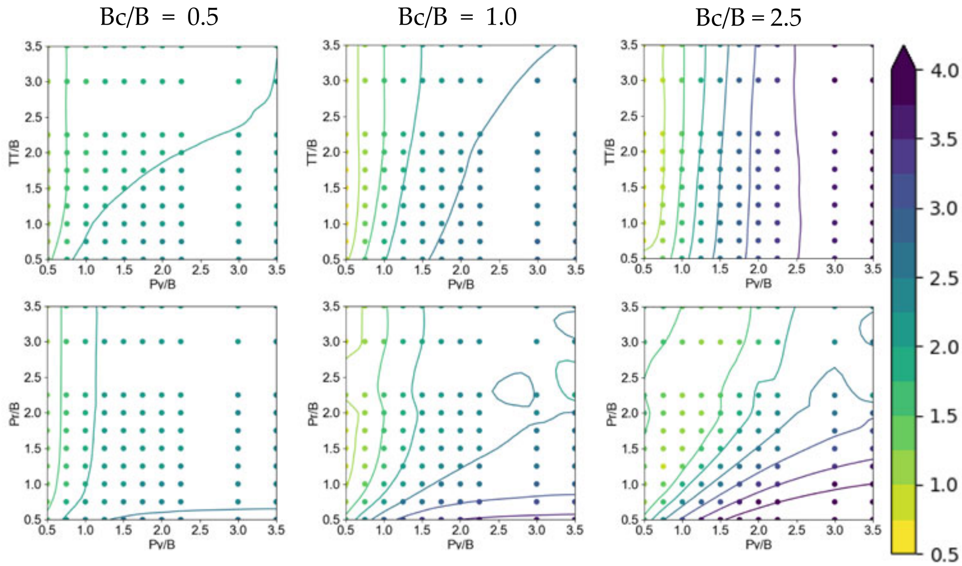

Two separate simulation batches were run to elucidate the relative effects of tension twinning as well as dislocation glide and climb slip modes on the high temperature flow. The first batch varied the tension twinning, <c + a> glide, and basal climb critical stresses (Fig. 4a–c). It is clear that climb of basal <a> dislocations is an important mechanism in the high temperature deformation of ZK10, as soft basal climb (Fig. 4a) is required to lower the residual error. As basal climb is deactivated by raising its relative critical stress (Figs. 4b and c), the total error becomes more dependent on the CRSS value of < c + a> slip. The simulations performed here suggest a very low CRSS ratio of <c + a> to basal glide (<1), which is physically unrealistic. This is most likely due to the exceptionally low r-values measured ($\sim$0.7), since < c + a> slip is known for lowering the strain anisotropy in textured Mg alloy sheets. Given the fact that the twin volume fraction is less than 7.5% at any temperature, it is not surprising that the CRSS value of twinning does not strongly influence the error. A second batch of simulations was used to highlight the relationship between basal climb and non-basal glide. Again, soft basal climb caused the total error to be nearly independent of prism and <c + a> glide strength (Fig. 4d). Again, when the critical stress ssfor basal climb is increased, soft <c + a> glide is required in order to achieve a lower total error (Fig. 4e and f). Curiously, the CRSS value controlling prism slip plays a minor role in influencing the total residual error in these high temperature simulations.

The optimal CRSS values of twinning, non-basal glide and climb relative to that of basal glide were used in Fig. 5 to illustrate the best-fit set of parameters to describe the high temperature deformation of ZK10. The absolute values of the Voce hardening parameters τ_o and τ_1 were varied to match experimental stress–strain curves. It would appear that <c + a> glide is the dominant mechanism during high temperature deformation, which would account for the exceptionally low r-values. Regardless, climb and glide of basal <a> dislocations still accommodate a significant

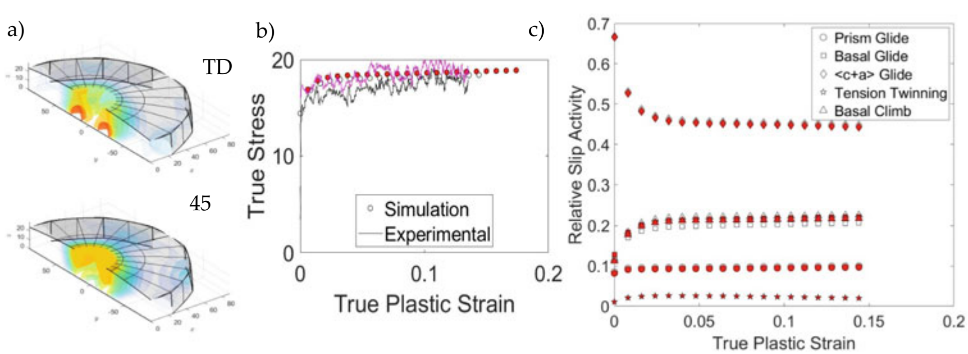

Fig. 5 High temperature-optimized simulations of **a** TD and 45° orientations textures. **b** Experimental and simulated stress–strain curves of TD and 45° samples. **c** Relative slip activity plots of simulated tensile tests. Closed symbols and lighter lines represent TD samples and opened symbols and darker lines represent 45° samples. (Color figure online)

amount of strain ($\sim 20\%$ each), which runs counter to traditional beliefs in climb and glide models for creep which stipulate that an overwhelming majority of strain occurs due to dislocation glide.

Conclusions

Measurements of the flow stress, r-values, and texture evolution during TD and 45° tension of basal textured Mg alloy ZK10 sheets have revealed three behavioral regimes corresponding to low ($Z < 22$), intermediate ($22 \le Z \le 35$), and high ($Z > 35$) temperature-compensated strain rates. Simple constitutive modeling reveals the behavior within each of these regimes to be characteristic of power-law creep, power-law breakdown, and thermally activated plasticity, respectively. Within the high Z, thermally activated plasticity regime, non-basal slip of <a> dislocations is shown to prevail, since it is required to produce the characteristic node-like textures. However, the low r-values ~ 1.5 appear to be due to increased <c + a> glide activity, relative to what is observed in alloy AZ31B. The contribution of twinning to in-plane tensile deformation was ultimately revealed to be minimal regardless of Z-value.

A new crystal plasticity model, which incorporates the strain and reorientation characteristics of dislocation climb is used to show that the transitions in both the r-value and texture evolution can be described if one accounts for the climb of basal <a> dislocations. These results continue to emphasize the role which dislocation climb has in strain accommodation and texture evolution, whereas prior work relegated climb to a role of dislocation recovery alone.

Acknowledgements The authors would like to thank the United States National Science Foundation, Division of Materials Research, Metals and Metallic Nanostructures (NSF-DMR-MMN) program, Grant No. 1810197, overseen by program manager Dr. Judith Yang, for financial support of this research. The authors would also like to thank Ricardo Lebensohn of Los Alamos National Laboratory for sharing the version of the VPSC code which was used to perform the simulations reported herein.

References

1. A. Chapuis and J. H. Driver, "Temperature dependency of slip and twinning in plane strain compressed magnesium single crystals," *Acta Mater.*, vol. 59, no. 5, pp. 1986–1994, 2011, https://doi.org/10.1016/j.actamat.2010.11.064.
2. T. Walde and H. Riedel, "Modeling texture evolution during hot rolling of magnesium alloy AZ31," *Mater. Sci. Eng. A*, vol. 443, no. 1–2, pp. 277–284, 2007, https://doi.org/10.1016/j.msea.2006.09.028.
3. A. Chapuis and Q. Liu, "Investigating the temperature dependency of plastic deformation in a Mg-3Al-1Zn alloy," *Mater. Sci. Eng. A*, vol. 725, no. March, pp. 108–118, 2018, https://doi.org/10.1016/j.msea.2018.04.019.
4. A. Jain and S. R. Agnew, "Modeling the temperature dependent effect of twinning on the behavior of magnesium alloy AZ31B sheet," *Mater. Sci. Eng. A*, vol. 462, no. 1–2, pp. 29–36, 2007, https://doi.org/10.1016/j.msea.2006.03.160.
5. K. Y. Xie, Z. Alam, A. Caffee, and K. J. Hemker, "Pyramidal i slip in c-axis compressed Mg single crystals," *Scr. Mater.*, vol. 112, pp. 75–78, 2016, https://doi.org/10.1016/j.scriptamat.2015.09.016.
6. J. Bohlen, M. R. Nürnberg, J. W. Senn, D. Letzig, and S. R. Agnew, "The texture and anisotropy of magnesium-zinc-rare earth alloy sheets," *Acta Mater.*, vol. 55, no. 6, pp. 2101–2112, 2007, https://doi.org/10.1016/j.actamat.2006.11.013.
7. F. Wang and S. R. Agnew, "Dislocation transmutation by tension twinning in magnesium alloy AZ31," *Int. J. Plast.*, vol. 81, pp. 63–86, 2016, https://doi.org/10.1016/j.ijplas.2016.01.012.
8. M. Ritzo, R. Lebensohn, L. Capolungo, and S. and Agnew, "Accounting for the effect of dislocation climb-mediated flow on the anisotropy and texture evolution of Mg alloy, AZ31B," *Int. J. Plast.*, 2021. In preparation.
9. R. A. Lebensohn, C. S. Hartley, C. N. Tome, and O. Castelnau, "Modeling the mechanical response of polycrystals deforming by climb and glide," *Philos. Mag.*, vol. 90, no. 5, pp. 567–583, 2010, https://doi.org/10.1080/14786430903213320.
10. R. A. Lebensohn, R. A. Holt, A. Caro, A. Alankar, and C. N. Tomé, "Improved constitutive description of single crystal viscoplastic deformation by dislocation climb," *Comptes Rendus - Mec.*, vol. 340, no. 4–5, pp. 289–295, 2012, https://doi.org/10.1016/j.crme.2012.02.011.
11. A. Izadbakhsh, K. Inal, R. K. Mishra, and M. Niewczas, "New crystal plasticity constitutive model for large strain deformation in single crystals of magnesium," *Comput. Mater. Sci.*, vol. 50, no. 7, pp. 2185–2202, 2011, https://doi.org/10.1016/j.commatsci.2011.02.030.
12. G. Proust, C. N. Tomé, A. Jain, and S. R. Agnew, "Modeling the effect of twinning and detwinning during strain-path changes of magnesium alloy AZ31," *Int. J. Plast.*, vol. 25, no. 5, pp. 861–880, 2009, https://doi.org/10.1016/j.ijplas.2008.05.005.
13. H. R. W. U.F. Kocks, C. N. Tome, "Texture And Anisotropy: Preferred Orientations in Polycrystals and Their Effect on Materials Properties." pp. 1–676, 1998.
14. A. Arsenlis and D. M. Parks, "Crystallographic aspects of geometrically-necessary and statistically-stored dislocation density," *Acta Mater.*, vol. 47, no. 5, pp. 1597–1611, 1999, https://doi.org/10.1016/S1359-6454(99)00020-8.
15. U. F. Tome, C N, Lebensohn, R A, Kocks, "A model for texture development dominated by deformation twinning: application to zirconium alloys," *Acta Mater.*, vol. 39, no. Ii, pp. 2667–2680, 1991.
16. H. Wang, P. D. Wu, J. Wang, and C. N. Tomé, "A crystal plasticity model for hexagonal close packed (HCP) crystals including twinning and de-twinning mechanisms," *Int. J. Plast.*, vol. 49, pp. 36–52, 2013, https://doi.org/10.1016/j.ijplas.2013.02.016.
17. S. R. Agnew and Ö. Duygulu, "Plastic anisotropy and the role of non-basal slip in magnesium alloy AZ31B," *Int. J. Plast.*, vol. 21, no. 6, pp. 1161–1193, 2005, https://doi.org/10.1016/j.ijplas.2004.05.018.
18. F. Bachmann, R. Hielscher, and H. Schaeben, "Texture analysis with MTEX- Free and open source software toolbox," *Solid State Phenom.*, vol. 160, pp. 63–68, 2010, https://doi.org/10.4028/www.scientific.net/SSP.160.63.
19. C. M. Sellars and W. J. M. Tegart, "Hot Workability," *Int. Metall. Rev.*, vol. 17, no. 1, pp. 1–24, Jan. 1972, https://doi.org/10.1179/imtlr.1972.17.1.1.
20. S. Ando, N. Harada, M. Tsushida, H. Kitahara, and H. Tonda, "Temperature Dependence of Deformation Behavior in Magnesium and Magnesium Alloy Single Crystals," *Key Eng. Mater.*,

vol. 345–346, pp. 101–104, 2007, https://doi.org/10.4028/www.scientific.net/kem.345-346.101.

21. S. Ando, H. Rikihisa, M. Tsushida, and H. Kitahara, "Activities of non-basal slips in deformation of magnesium alloy single and poly crystals," *Mater. Sci. Forum*, vol. 941 MSF, pp. 1242–1247, 2018, https://doi.org/10.4028/www.scientific.net/MSF.941.1242.
22. S. Ando, A. Kodera, K. Fukushima, M. Tsushida, and H. Kitahara, "Tensile deformation of magnesium and magnesium alloy single crystals," *Mater. Sci. Forum*, vol. 783–786, pp. 341–345, 2014, https://doi.org/10.4028/www.scientific.net/msf.783-786.341.
23. S. Ando, M. Tsushida, and H. Kitahara, "Deformation behavior of magnesium single crystal in c-axis compression and a-axis tension," *Mater. Sci. Forum*, vol. 654–656, October, pp. 699–702, 2010, https://doi.org/10.4028/www.scientific.net/MSF.654-656.699.